European Journal of Pharmacology 760 (2015) 154–162

Contents lists available at ScienceDirect

European Journal of Pharmacology

journal homepage: www.elsevier.com/locate/ejphar

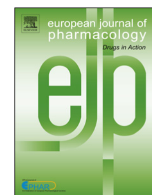

Molecular and cellular pharmacology

Biochemical characterization and molecular dynamic simulation of β-sitosterol as a tubulin-binding anticancer agent

Tejashree Mahaddalkar [a], Charu Suri [b], Pradeep Kumar Naik [b], Manu Lopus [a,*]

[a] Experimental Cancer Therapeutics and Chemical Biology, Department of Biology, UM-DAE Centre for Excellence in Basic Sciences, Kalina, Santacruz (E), Mumbai 400098, India

[b] Department of Biotechnology and Bioinformatics, Jaypee University of Information Technology, Waknaghat, Solan 173234, Himachal Pradesh, India

ARTICLE INFO

Article history:
Received 15 December 2014
Received in revised form
19 March 2015
Accepted 8 April 2015
Available online 23 April 2015

Chemical compounds studied in this article:
Beta-sitosterol (PubChem CID: 222284)
Colchicine (PubChem CID: 6167)
Taxol (PubChem CID: 36314)
Vinblastine sulfate (PubChem CID: 241902)
8-anilinonaphthalene-1-sulfonic acid (PubChem CID: 1369)
5,5′-Dithiobis(2-nitrobenzoic acid) (PubChem CID: 6254)
Guanosine 5′-triphosphate (PubChem CID: 6830)

Keywords:
Beta-sitosterol
Tubulin
Microtubule
Cancer
Molecular dynamic simulation

ABSTRACT

Beta-sitosterol (β-SITO), a phytosterol present in pomegranate, peanut, corn oil, almond, and avocado, has been recognized to offer health benefits and potential clinical uses. β-SITO is orally bioavailable and, as a constituent of edible natural products, is considered to have no undesired side effects. It has also been considered as a potent anticancer agent. However, the molecular mechanism of action of β-SITO as a tubulin-binding anticancer agent and its binding site on tubulin are poorly understood. Using a combination of biochemical analyses and molecular dynamic simulation, we investigated the molecular details of the binding interactions of β-SITO with tubulin. A polymer mass assay comparing the effects of β-SITO and of taxol and vinblastine on tubulin assembly showed that this phytosterol stabilized microtubule assembly in a manner similar to taxol. An 8-anilino-1-naphthalenesulfonic acid assay confirmed the direct interaction of β-SITO with tubulin. Although β-SITO did not show direct binding to the colchicine site on tubulin, it stabilized the colchicine binding. Interestingly, no sulfhydryl groups of tubulin were involved in the binding interaction of β-SITO with tubulin. Based on the results from the biochemical assays, we computationally modeled the binding of β-SITO with tubulin. Using molecular docking followed by molecular dynamic simulations, we found that β-SITO binds tubulin at a novel site (which we call the 'SITO site') adjacent to the colchicine and noscapine sites. Our data suggest that β-SITO is a potent anticancer compound that interferes with microtubule assembly dynamics by binding to a novel site on tubulin.

© 2015 Elsevier B.V. All rights reserved.

1. Introduction

Phytochemicals from natural sources, such as vegetables, fruits, herbs, and tea, are known to possess cancer preventive properties and cancer treatment potential (Saha and Khuda-Bukhsh, 2013). Beta-sitosterol (β-SITO) is a major plant sterol present in pomegranate, peanut, olive oil, corn oil, avocado, and almonds, and in different quantities in a number of vegetables, fruits and legumes (Jiménez-Escrig et al., 2006; Rosenblat et al., 2013). This sterol regulates blood cholesterol levels (Wu et al., 2014) and is anti-atherogenic (Rosenblat et al., 2013), anti-diabetic (Radika et al., 2013), and anti-asthmatic (Yuk et al., 2007). Previous studies on the anticancer properties of β-SITO indicated that it could also be a potential anticancer drug. For example, a study carried out using breast cancer cells showed that β-SITO activates Fas signaling and induces apoptosis (Vundru et al., 2013). β-SITO was found to be effective at killing colon (HT-29) and prostate (LNCaP) cancer cell lines (Awad et al., 1996; von Holtz et al., 1998). Importantly, a study by Baskar et al. (2010) found that the compound can be selectively toxic to cancer cells without causing considerable damage to normal cells. A report by Moon et al. (2008) demonstrated that the sterol can arrest cells at G_2/M and affect microtubule assembly. Considering the drawbacks of current anticancer drugs, such as intolerable, toxic side effects, β-SITO appears to be a promising alternative. In this context, it is relevant to note that this phytosterol has neuroprotective properties (Hamedi et al., 2014).

Microtubules, which are cylindrical polymers of the protein tubulin, form a major structural component of cytoskeleton in eukaryotes. Tubulin is composed of two non-identical subunits, α and β. The structural integrity of tubulin is essential for the formation of functional mitotic spindle that can properly segregate sister chromosomes during cell division. Tubulin provides binding

* Corresponding author. Tel.: +91 773 849 0187.
E-mail address: manu.lopus@cbs.ac.in (M. Lopus).

http://dx.doi.org/10.1016/j.ejphar.2015.04.014
0014-2999/© 2015 Elsevier B.V. All rights reserved.

sites for a variety of anticancer compounds, several of which have progressed to clinical use as approved anticancer drugs. For example, United States Food and Drug Administration-approved drugs such as ixabepilone (Ixempra, Bristol-Myers Squibb; http://www.accessdata.fda.gov/drugsatfda_docs/label/2009/022065s002lbl.pdf), eribulin (Halaven, Eisai Co.; http://www.accessdata.fda.gov/drugsatfda_docs/label/2010/201532lbl.pdf) and the maytansinoid used for the antibody drug conjugate ado-trastuzumab emtansine (Kadcyla,Genentech; http://www.accessdata.fda.gov/drugsatfda_docs/label/2013/125427lbl.pdf) target tubulin and microtubules through diverse molecular mechanisms, thereby inhibiting tumor progression. Despite accumulating evidence of β-SITO's anticancer properties, little is known about its molecular mechanism of action or putative binding site on tubulin. A study conducted approximately a decade ago first reported β-SITO's possible effects on microtubules (Wang et al., 2006). A more recent study provided evidence that β-SITO affects tubulin assembly and induces G_2/M arrest (Moon et al., 2008).

We investigated the molecular details of the binding interaction of β-SITO with tubulin using a combination of biochemical analyses, and molecular dynamic simulations (MD simulations). We found that β-SITO stabilized microtubule assembly and showed direct binding to tubulin. While not binding to the colchicine site itself, β-SITO stabilized colchicine binding to tubulin. Interestingly, β-SITO's interactions with tubulin did not involve the sulfhydryl groups of tubulin. Based on these findings, a comprehensive molecular modeling study was performed, using a combination of ligand docking and MD simulations. The modeling data substantiated the biochemical findings and indicated the presence of a unique binding site for β-SITO on tubulin at the intra-dimer interface, distinct from the colchicine site.

2. Materials and methods

2.1. Materials

Beta-sitosterol (β-SITO), vinblastine, taxol, 8-anilino-1-naphthalenesulfonic acid (ANS), Guanosine-5′-triphosphate (GTP), Piperazine-N,N′-bis(2-ethanesulfonic acid) (Pipes), Magnesium sulfate ($MgSO_4$), Ethylene glycol tetraacetic acid (EGTA), and 5,5′-dithiobis-2-nitrobenzoic acid (DTNB) were purchased from Sigma (St. Louis, MO). All other reagents were of analytical grade. β-SITO was dissolved in dimethyl formamide (DMF) after purging the latter with argon. Vinblastine was dissolved in water. Taxol was dissolved in dimethyl sulfoxide (DMSO).

2.2. Spectral measurements

Fluorescence spectra were obtained using a Flouromax 4 spectrofluorometer (Horiba Scientific, Edison, NJ) supported by a FluorEssence 3.5 software. A 0.3 cm quartz cuvette was used for reading the samples. Absorbance readings were taken in a Tecan Infinite® M200 PRO multimode reader (Tecan, Switzerland).

2.3. In vitro tubulin polymerization assay

Tubulin was purified from goat brain as described (Gupta and Panda, 2002), and stored at −80 °C until used. The tubulin was polymerized without or with different concentrations of β-SITO (0–20 μM), 1 μM vinblastine, or 5 μM taxol in PEM buffer (50 mM Pipes, 1 mM EGTA, 3 mM $MgSO_4$, pH 6.8), in the presence of 1 M glutamate, at 35 °C, for 45 min. The polymers were centrifuged in a Beckman Coulter Aventi J/26 S XP centrifuge (Beckman Coulter, Brea, CA), using a JA-18.1 rotor (35000×g; 35 °C; 45 min). After the centrifugation, the supernatants were carefully aspirated off, and the pellets dissolved in water on ice by overnight incubation (Lopus et al., 2012). Next day, the protein concentrations were measured using a Bradford assay with bovine serum albumin (BSA) as the standard (Bradford, 1976).

2.4. Conformational states of tubulin tertiary structure using 8-anilino-1-naphthalenesulfonic acid (ANS)

ANS has been used to investigate whether a ligand makes direct contact with its target protein and alters the latter's structural features (Lopus and Panda, 2006). Tubulin (2 μM) was incubated with β-SITO (0–50 μM) for 30 min at 35 °C. After the incubation, ANS (50 μM) was added and the samples were incubated for an additional 20 min. Subsequently, the samples were excited at 380 nm and the emission spectra were collected (390–500 nm).

2.5. Colchicine binding assay

To obtain structural insights into putative binding site of β-SITO on tubulin, we tested whether the compound binds at the colchicine binding site, a site shared by compounds such as colchicine, podophyllotoxin, combreastatin, and curacin A (Lu et al., 2012; Bhattacharyya and Wolff, 1974). Tubulin (3 μM) was incubated with different concentrations (0–50 μM) of β-SITO at 35 °C for 30 min. Subsequently, colchicine (10 μM) was added and the samples were incubated for an additional 60 min at 35 °C. The samples were excited at 360 nm, and the emission spectra were recorded (390–460 nm).

2.6. 5,5′-dithiobis-2-nitrobenozoic acid (DTNB) assay

5,5′-dithiobis-2-nitrobenozoic acid (DTNB) reacts specifically with sulfhydryl groups and releases 3-thio-6-nitrobenzoate ion that absorbs light at 412 nm (Roychowdhury et al., 2000). Potential modification of sulfhydryl groups by the treated ligand can be monitored by measuring changes in the absorbance at 412 nm (Roychowdhury et al., 2000). Tubulin (3 μM) was incubated with different concentrations of β-SITO (0–75 μM) for 15 min at 35 °C in 20 mM phosphate buffer. Subsequently, DTNB (200 μM) was added and the samples were incubated for 45 min at 35 °C. Absorbance was measured at 0 min and after the 45 min incubation. The number of modified cysteine residues was calculated by using molar extinction coefficient of 13 600 M^{-1} cm^{-1} for DTNB at 412 nm.

2.7. Molecular modeling

2.7.1. Molecular building of β-SITO and structure optimization

Molecular structure of β-SITO was built using molecular builder of Maestro (version 9.2, Schrödinger). Energy minimization of the structure was performed using Macromodel software (version 9.9, Schrödinger), and by OPLS (Optimized Potentials for Liquid Simulations) 2005 force field with PRCG (periodic ranging code group) algorithm (1000 steps of minimization, energy gradient, 0.001). Ligprep software (version 2.5, Schrödinger, LLC) was used for assigning appropriate bond order to the molecular structure. Geometrical optimization of the β-SITO structure was carried out using hybrid density functional theory (DFT) with Becke's three-parameter exchange potential and the Lee–Yang–Parr (B3LYP) correlation functional (Lee et al., 1988; Becke, 1993). 3–21 G* was used as basis set (Binkley et al., 1980). Jaguar software (version 7.7, Schrödinger, LLC) was used for the final geometrical optimization of β-SITO.

2.7.2. Preparation of crystal structure of αβ-tubulin complex

The X-ray crystallographic structure of αβ-tubulin complex (PDB ID: 1SA0, resolution 3.58 Å) was prepared as reported earlier (Manchukonda et al., 2013). All-atom molecular dynamic simulation in explicit water was carried out using GROMACS 4.5 and

AMBER99SB force field for 10 ns for additional stabilization of the structure. Five thousand frames were generated in the MD trajectories, and the last 2000 frames were used to generate an average structure of the tubulin complex. The overall quality of the model, stereochemical values, and non-bonded interactions were evaluated using PROCHECK, ERRAT and VERIFY 3D. PROCHECK indicated that 94.8% of backbone angles were in allowed regions (*G*-factors, −0.12). The ERRAT score, 88.402, and VERIFY 3D score, 95.25%, substantiated that the model is a good quality one.

2.7.3. Prediction and analysis of β-SITO binding pocket

All possible binding sites of β-SITO on tubulin heterodimer were predicted and analyzed using SiteMap software (version 2.4, Schrodinger), which uses Goodford's grid algorithm (Goodford, 1985) to define a binding site with a set of site points. For comparative analyzes, only those binding sites that consist of at least 5 site points were considered.

2.7.4. Molecular docking of β-SITO to tubulin heterodimer

The receptor-grid file was generated using a grid receptor generation program (van der Waals scaling, 0.4 Å; absolute partial charges, ≤0.25 to atoms of protein). Using Glide 5.7 (Schrodinger, LLC), grid boxes of 12 Å each for the bounding and enclosing boxes were produced at the centroid of the predicted binding sites. Molecular docking of the optimized β-SITO structure onto tubulin was performed using Glide XP 4.5, and was evaluated using a Glide XP_{Score} function (Halgren et al., 2004; Friesner et al., 2004). Initially, fifty thousand poses were sampled and 4000 among them were subjected to energy minimization (conjugate gradients method over 1000 steps). Finally, 30 structures with lowest energy conformations were screened for favorable Glide docking score. Single best conformation for β-SITO–tubulin complex was then selected for further molecular modeling calculations.

2.7.5. Molecular dynamics simulations (MD simulations)

The docked complex of β-SITO with tubulin was used as initial conformation for MD simulation, which was performed with an AMBER 11.0 software suite using AMBER99SB force field. Each molecular system was solvated with ~32,300 TIP3P water molecules in a truncated octahedral box and neutralized by adding 32 Na^+ ions. Energy minimization of the molecular system was done in three consecutive rounds (each consisting of 500 steps of steepest descent followed by 500 steps of a conjugate gradient energy minimization method). By employing this method, bad contacts in the structure were removed. Positional restraints were applied to the whole system for the first and second round, to allow for relaxation of the solvent molecules (Force constants, 10 $kcal^{-1}Å^{-2}$ and 2 $kcal^{-1}Å^{-2}$, respectively). In the third round, the whole system was minimized without restraint. This was followed by a 10 ns MD simulation with a time step of 2 fs following 200 ps of equilibration at 300 K. SHAKE algorithm (Ryckaert et al., 1977) was applied for every bond involving hydrogen bonds. The non-bonded cut off distance was 10 Å. Particle Mesh Ewald (PME) method was applied to treat long-range electrostatic interactions. A langevin thermostat was used to regulate the temperature of the system. For carrying out all equilibration and ensuing MD stages, an isothermal isobaric (NPT) ensemble (Berendsen barometer; Hornak et al., 2006; Berendsen et al., 1984; target pressure, 1 bar) was used, and trajectories were recorded at every 1 ps.

2.7.6. Calculation of binding free energy of β-SITO with tubulin using molecular mechanic/ Poisson–Boltzmann surface area (MM–PBSA) and molecular mechanics with generalized born /surface area (MM–GBSA) solvation

Binding free energy of β-SITO with tubulin was calculated based on both MM–PBSA and MM–GBSA [Kollman et al., 2000; Massova and Kollman, 2000) using AMBER 11.0. For this, a total of 1000 snapshots, generated from the last 2 ns of the MD trajectory, were considered. The binding free energy (ΔG_{bind}) of β-SITO for each frame was then calculated using the following equation:

$$\Delta G_{bind} = G_{complex} - (G_{receptor} + G_{ligand}) \quad (1)$$

The free energy (*G*) for each species was calculated as described previously, using the MM–PBSA and MM–GBSA methods. Specifically

$$G = E_{gas} + G_{sol} - TS \quad (2)$$

$$E_{gas} = E_{int} + E_{ele} + E_{vdw} \quad (3)$$

$$G_{ele,PB(GB)} = E_{ele} + G_{PB(GB)} \quad (4)$$

$$G_{sol} = G_{sol-np} + G_{PB(GB)} \quad (5)$$

$$G_{sol-np} = \gamma SAS$$

where E_{gas} is the gas-phase energy; E_{int} is the internal energy; and E_{ele} and E_{vdw} are the Coulomb and van der Waals energies, respectively. AMBER ff99SB molecular mechanics force field was used to calculate E_{gas}. The solvation free energy, $G_{sol,}$ was decomposed into polar and non-polar contributions. Solving the PB and GB equation provided the polar solvation contribution, $G_{PB(GB)}$. $G_{ele,PB(GB)}$ and G_{sol-np} are polar and the non-polar solvation contributions. *T* and *S* are the temperature and the total solute entropy, respectively.

2.7.7. Ligand–residue interaction decomposition

The binding free energy contribution of each residue with the β-SITO within the binding cavity of αβ tubulin dimer was analyzed using MM–GBSA decomposition process utilizing MM–GBSA module in Amber 11.0. The binding free energy of each ligand–residue pair includes three energy terms: the van der Waals contribution (ΔE_{vdw}), the electrostatic contribution (ΔE_{ele}) and the solvation contribution (ΔE_{sol}). All the energy components were calculated using the same frames obtained from MD trajectories that were used for calculation of binding energy of β-SITO.

3. Results

3.1. β-SITO promoted microtubule assembly

The majority of the microtubule-targeted agents either promotes or inhibits tubulin assembly. We tested the effect of β-SITO on microtubule assembly using a polymer mass assay, in which the microtubules, formed in the absence or presence of different concentrations of β-SITO, were collected by centrifugation followed by determination of the concentration of the sedimented polymers using a Bradford assay. β-SITO (Fig. 1A) stabilized microtubules assembly (Fig. 1B). Compared to control, β-SITO showed an increase in the assembled polymer in a concentration-dependent manner. Specifically, compared to control, 10 μM and 20 μM β-SITO increased the polymer mass by 7% and 23%, respectively (Fig. 1B). The increase in polymer mass at 20 μM β-SITO was comparable to that of the polymers formed in the presence of 5 μM taxol (the latter increased the polymer mass by 26%). One μM vinblastine showed a 32% reduction in the net polymer mass, compared to control. The data indicate that β-SITO does not inhibit microtubule assembly, and instead, it is a potential stabilizer and promoter of microtubule assembly.

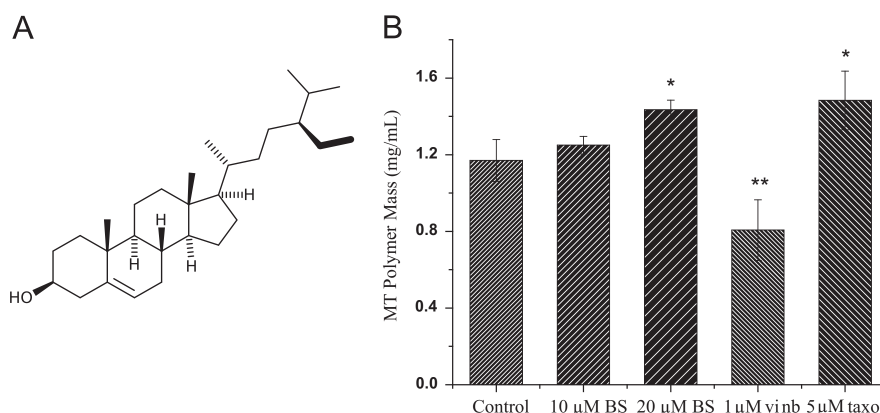

Fig. 1. β-SITO, and its effects on microtubule polymer mass. (A) Structure of β-SITO (3S,8S,9S,10R,13R,14S,17R)-17-[(2R,5R)-5-ethyl-6-methylheptan-2-yl]-10,13-dimethyl-2,3,4,7,8,9,11,12,14,15,16,17-dodecahydro-1 H-cyclopenta[a]phenanthren-3-ol). (B) Effect of β-SITO on microtubule polymer mass. Tubulin (15 μM) was assembled without or with β-SITO (0–20 μM), vinblastine (1 μM), or taxol (5 μM) (35 °C, 45 min) and the assembled polymers sedimented (35 °C, 45 min). Concentration of the polymers was determined using a Bradford assay. β-SITO enhanced the quantity of sedimented polymers, indicating potential stabilization of microtubule assembly. The experiment was repeated twice. Data represent mean ± S.D.$^{*}P<0.05$, versus control; $^{**}P<0.01$, versus control (Students' *t*-test).

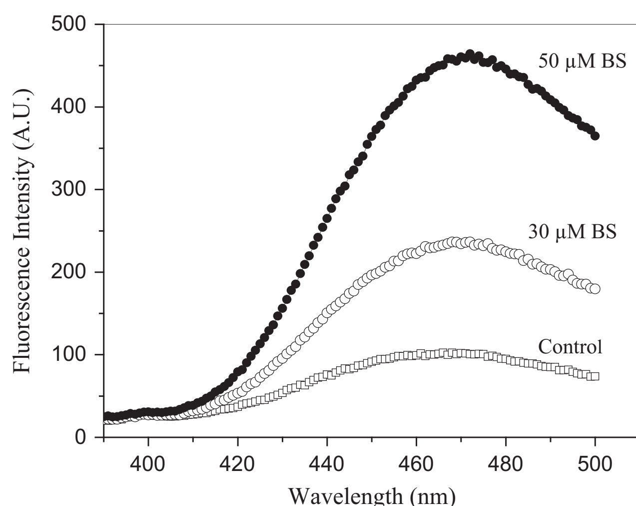

Fig. 2. Enhancement of tubulin-ANS fluorescence by β-SITO. Tubulin (2 μM) was incubated (35 °C, 30 min) without (open squares) or with 30 μM (open circles), or 50 μM (solid circles) β-SITO, followed by an additional 20 min incubation with ANS (50 μM). The samples were excited at 380 nm and the emission spectra collected (390–500 nm). β-SITO showed a concentration-dependent increase in tubulin-ANS fluorescence, indicating its binding to tubulin. The graph is a representative of three independent experiments.

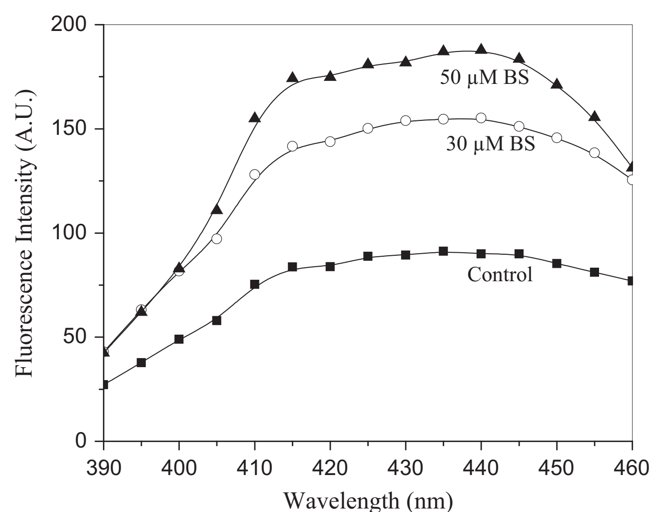

Fig. 3. Stabilization of colchicine binding to tubulin by β-SITO. Tubulin (3 μM) was incubated (35 °C, 30 min) without (solid squares), or with 30 μM (open circles) or 50 μM (sold triangles) β-SITO. Subsequently, the samples were incubated (35 °C, 1 h) with colchicine (10 μM). Following the incubation, the samples were excited at 360 nm, and the emission spectra recorded (390 nm – 460 nm). β-SITO increased the tubulin-colchicine fluorescence, indicating the stabilization of colchicine binding to tubulin. The graph is a representative of three independent experiments.

3.2. *β-SITO altered the surface features of tubulin*

β-SITO perturbed the tertiary structure of tubulin as indicated by the increase in tubulin-ANS fluorescence with increasing concentrations of β-SITO. Compared to control, 30 μM and 50 μM of β-SITO increased the ANS fluorescence considerably (Fig. 2). Specifically, at 470 nm, 30 μM β-SITO increased the tubulin-ANS fluorescence by 16%, and 50 μM β-SITO showed a 40% increase in the fluorescence, indicating that β-SITO interacts with tubulin and alters the surface features of the protein.

3.3. *β-SITO did not bind colchicine site on tubulin*

Colchicine binding site on tubulin provides binding site for several anticancer agents including colchicine, podophyllotoxin, combreastatin, and curacin A (Lu et al., 2012). Colchicine in aqueous solution does not show considerable fluorescence. However, tubulin-bound colchicine shows substantial increase in fluorescence intensity (Bhattacharyya and Wolff, 1974). Using this colchicine-binding assay, we examined if β-SITO binds at colchicine site. A pre-incubation of tubulin with β-SITO (10–50 μM) did not show any decrease in colchicine fluorescence. Interestingly, at 30 μM and 50 μM, β-SITO showed a slight but consistent increase in tubulin-colchicine fluorescence, indicating that the β-SITO does not bind colchicine directly, but stabilizes colchicine binding (Fig. 3).

3.4. *β-SITO did not modify the sulfhydryl groups of tubulin*

Tubulin binding agents such as vinblastine and colchicine are known to modify cysteine residues of proteins (Roychowdhury et al., 2000). When tubulin was incubated with different concentrations of β-SITO (0–75 μM), followed by incubation with DTNB (200 μM), there was no reduction in the number of cysteine residues. Conversely, we found a slight increase in the number of cysteine residues in the presence of β-SITO. For example, whereas in the absence of β-SITO the number of accessible cysteine residues was 15 ± 1, in the presence of 75 μM β-SITO, the number

of available cysteine residues was found to be 17 ± 0.7 (Table 1). The result suggests that the binding of β-SITO to tubulin does not involve sulfhydryl residues of tubulin.

3.5. Computational modeling of the interactions of β-SITO with tubulin indicated a unique binding site near the colchicine site

Based on the findings from the biochemical assays, we investigated the molecular details of the binding of β-SITO with tubulin using ligand docking and molecular dynamic simulation approaches.

3.5.1. Beta SITO binds to tubulin with strong affinity

The molecular interaction and binding affinity of β-SITO with αβ-tubulin were determined using molecular docking and MM–PBSA/MM–GBSA calculations. A blind docking approach was employed to examine the molecular docking of β-SITO with tubulin in which β-SITO was docked into each of the predicted binding sites. The probable binding site of β-SITO was then screened based on the better docking scores and findings from biochemical experiments, which indicated the stabilization of the colchicine site and the non-involvement of Cys residues in β-SITO-tubulin interaction (Fig. 3 and Table 1, respectively). Among the docking scores of β-SITO for all the binding sites (Table 2), binding site 4, with which β-SITO had the best docking score (−7.694 kcal/mol) and which had no –SH groups within an 8 Å diameter, was selected as the putative binding site.

Table 1
Effect of β-SITO on Cys residues of tubulin.

β-SITO (μM)	Number of Cys residues
0	15 ± 1
50	16 ± 1
75	17 ± 0.7

Based on the insights from molecular docking, we used molecular dynamics simulations to determine the preferential binding mode of β-SITO with αβ-tubulin complex. The complex obtained from molecular docking was simulated for 10 ns to obtain a total of 10,000 frames. The stability of the system was monitored by the root-mean-square deviation (RMSD) of Cα-atoms throughout the duration of the simulation as shown in Fig. 4. The RMSD of the complex reached equilibrium at 4000 ps, and the RMSDs of the atoms oscillated between 1.5 Å and 2 Å afterwards. The compound was observed to dock at the αβ-tubulin complex throughout the 10 ns simulation. The binding mode of β-SITO was found to involve interactions with both α-tubulin and β-tubulin and was well accommodated inside the binding cavity (Fig. 5A and B). The physico-chemical properties of the interaction are shown in Table 2. The binding mode is represented in two

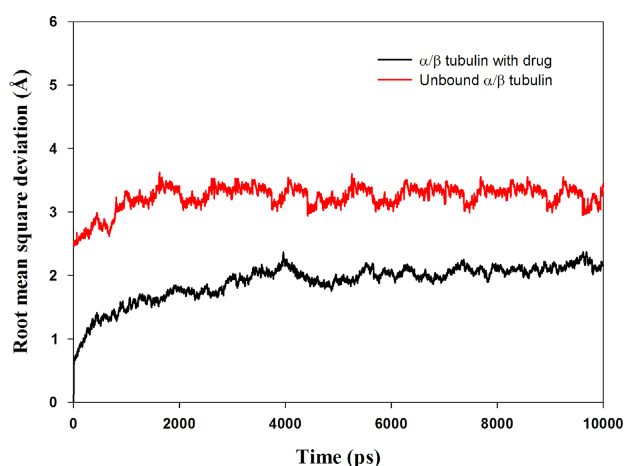

Fig. 4. Root mean square deviation of Cα atoms of α/β-tubulin in the free form and β-SITO bound form during MD simulation. The relative fluctuation in the RMSD of the Cα atoms was very small after 400 ps, indicating that each system reached equilibrium at 400 ps.

Table 2
Prediction of β-SITO binding site on tubulin.

Binding Site	Site Score	Size	Exposure	Enclosure	Contact	Phobic	Philic	Balance	Don/acc	Docking score (kcal/mol)
1	1.043	470	0.513	0.803	0.964	1.021	0.903	1.131	0.556	−8.793
2	1.017	226	0.517	0.745	0.924	1.05	0.862	1.219	0.826	−8.785
3	0.913	125	0.606	0.667	0.806	0.292	1.003	0.291	0.509	−6.016
4	**0.785**	**76**	**0.73**	**0.673**	**0.765**	**0.533**	**0.758**	**0.704**	**1.502**	**−7.694**
5	0.634	46	0.699	0.665	0.831	0.05	1.164	0.043	2.208	−6.289
6	0.733	44	0.604	0.63	0.848	1.692	0.629	2.691	1.207	−4.726
7	0.719	39	0.629	0.721	0.957	1.243	0.718	1.732	0.578	−5.527
8	0.507	33	0.822	0.565	0.646	0.423	0.603	0.702	1.933	−4.497
9	0.602	33	0.689	0.619	0.811	0.677	0.96	0.705	2.103	−6.105
10	0.551	25	0.658	0.654	0.855	0.318	0.771	0.413	2.328	−7.227
11	0.599	37	0.667	0.601	0.693	0.49	0.982	0.499	1.154	−3.324
12	0.591	22	0.699	0.699	0.969	0.724	0.896	0.808	0.562	−5.991
13	0.731	26	0.447	0.888	1.389	0.318	1.614	0.197	0.959	−6.114
14	0.467	22	0.821	0.602	0.723	0.007	1.024	0.007	1.163	−4.901
15	1.034	22	0.463	0.992	1.257	4.473	0.595	7.524	1.166	−2.361
16	0.565	18	0.746	0.672	0.86	1.243	0.525	2.369	0.778	−5.056
17	0.446	12	0.769	0.569	0.785	0.479	0.772	0.621	0.742	−2.318
18	0.747	15	0.444	0.99	1.539	0.53	1.584	0.335	1.026	−4.683
19	0.449	17	0.828	0.552	0.686	0.599	0.686	0.873	0.976	−3.502
20	0.36	9	0.873	0.515	0.661	0.197	0.741	0.266	5.582	−2.046
21	0.479	19	0.829	0.575	0.624	0.995	0.418	2.38	0.952	−4.189
22	1.058	9	0.25	0.999	1.739	8.431	0.103	81.674	0	−3.804
23	0.422	12	0.824	0.561	0.697	0.384	0.818	0.47	1.983	−4.819
24	0.388	16	0.828	0.492	0.542	0.19	0.78	0.244	0.739	−2.791
25	0.332	8	0.904	0.524	0.544	0.058	0.642	0.09	0.424	−3.804
26	0.373	10	0.848	0.527	0.703	0.003	0.93	0.004	3.209	−1.960
27	0.379	6	0.872	0.518	0.688	0.856	0.368	2.326	4.57	−3.922
28	0.597	6	0.727	0.814	1.289	0.944	0.996	0.948	1.716	−6.030

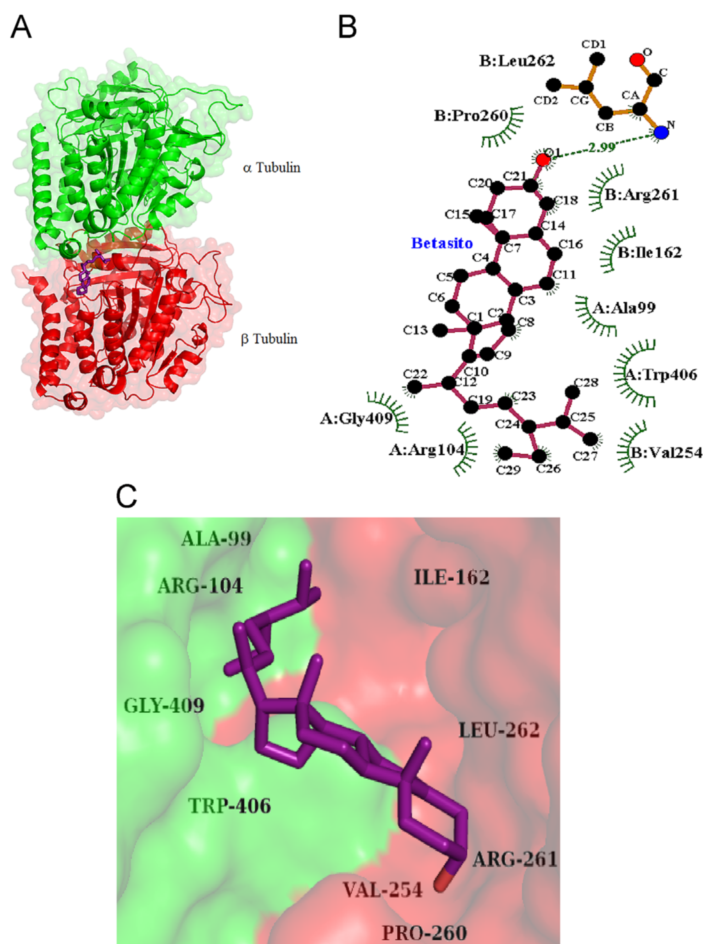

Fig. 5. β-SITO binds a novel site on tubulin. (A, B) Three dimensional representation of β-SITO (shown in purple on 5A)-tubulin interaction. Only the residues that contribute binding free energy less than −0.5 kcal/mol are shown. (C) Two-dimensional representation of the binding mode of β-SITO with tubulin, and the residues involved therein. 'A' denotes the residues of α-tubulin and 'B' denotes the residues of β-tubulin.

Table 3
Energy components and their energy contribution for the interactions between β-SITO and tubulin.

Energy component	Energy contribution (kcal/mol) 0
ΔE_{int}	
ΔE_{vdw}	−41.97
ΔE_{ele}	−7.849
$\Delta E_{gas}/\Delta E_{MM}$	−49.70
ΔG_{PB}	32.97
ΔG_{sol-np}	−3.839
$\Delta G_{solv,PB}$	29.13
$\Delta G_{ele,PB}$	25.12
$\mathbf{\Delta G_{bind,PB}}$	**−20.57**
ΔG_{GB}	23.55
$\Delta G_{solv,GB}$	19.13
$\Delta G_{ele\ GB}$	15.70
$\mathbf{\Delta G_{bind,GB}}$	**−30.57**

steps (Fig. 5B and C): (a) receptor residues that have strong interactions, such as hydrogen bonding with β-SITO; and (b) receptor residues that are close to the β-SITO but have weak or diffuse interactions with the ligand, such as hydrophobic interactions.

The predictive binding free energy of β-SITO with the αβ-tubulin complex was determined using a combination of MM–PBSA and MM–GBSA methods (see Table 3). The calculated binding energy, −20.57 kcal/mol (MM–PBSA) and −30.57 kcal/mol (MM–GBSA), indicates strong interactions of β-SITO with αβ-tubulin. The data

Table 4
Per residue energy decompositions ($\Delta G_{bind,GB}$ (kcal/mol)) in β-SITO–α/β-tubulin complex.

Chain	Residue	$\Delta E_{i,vdw}$	$\Delta E_{i,ele}$	$\Delta G_{i,sol\ GB}$	$\Delta G_{i,sol-np}$	$\Delta H_{i,tot,GB}$
A	ALA 99	−0.532	−0.001	0.1	−0.069	−0.502
	ARG 104	−1.679	0.148	0.793	−0.23	−0.969
	TRP 406	−3.001	−0.052	1.759	−0.452	−1.747
	GLY 409	−1.105	0.01	0.719	−0.243	−0.619
B	ILE 162	−0.418	0.017	−0.045	−0.133	−0.579
	VAL 254	−0.556	0.017	−0.022	−0.035	−0.595
	PRO 260	−1.471	−0.813	0.644	−0.257	−1.897
	ARG 261	−0.657	−1.079	1.18	−0.017	−0.574
	LEU 262	−0.836	−1.422	0.98	−0.109	−1.388

also suggest that both the intermolecular van der Waals (ΔE_{vdw}) and the electrostatic (ΔE_{ele}) interactions contributed significantly to the binding, whereas the polar solvation terms ($\Delta G_{PB(GB)}$) counteracted the binding. In contrast, non-polar solvation terms (ΔG_{sol-np}) —which correspond to the burial of solvent-accessible surface-area upon ligand binding—made only slightly favorable contributions. Although the gas-phase electrostatic value (ΔE_{gas}) was in favor of the binding of β-SITO, the overall electrostatic interaction energy ($\Delta G_{ele,PB(GB)}$) was positive and thus unfavorable for binding, perhaps due to the large desolvation penalty of charged and polar groups that are not sufficiently compensated by a complex formation. Comparing the net polar energy ($\Delta G_{PB(GB)}+\Delta E_{ele}$) and nonpolar energy ($\Delta G_{sol-nonpolar}+\Delta E_{vdw}$) contributions, we observed that the

binding of β-SITO to tubulin is driven mostly by nonpolar interaction. The binding free energy of individual amino acids involved in interactions with β-SITO was calculated based on MM–GBSA (Table 4). Nine residues contributed significant binding energy with β-SITO, each yielding < -0.5 kcal/mol of free energy. The analysis revealed that Trp 406 of α-tubulin and two residues, Pro 260 and Leu 262 of β-tubulin, contributed binding free energy of < -1.0 kcal/mol and are key residues in the binding of β-SITO.

4. Discussion

A major challenge associated with cancer chemotherapy is the toxic and often unbearable side effects of the drugs (Miltenburg and Boogerd, 2014). Therefore, identifying anticancer agents less toxic to normal cells and understanding their interactions with cellular targets are important in the development of effective cancer therapeutics. Through a literature survey, we identified β-SITO as a potent anticancer agent present in several edible vegetables and nuts (Jiménez-Escrig et al., 2006; Awad et al., 2000), whose health protective effects might prevent severe side effects in patients (see the introduction). Our study found that β-SITO is a tubulin binding agent and that its interaction with tubulin involves several interesting features.

4.1. Biochemical characterization of β-SITO-tubulin interaction

As observed with a polymer mass assay, β-SITO slightly promoted tubulin assembly (Fig. 1B). However, it required a concentration of 20 μM to produce a 23% increase in polymer mass, while Taxol needed only 5 μM to produce a similar effect, indicating that, as a promoter of tubulin assembly, β-SITO is approximately 4 times weaker than Taxol. Drugs that do not significantly alter microtubule polymer mass are considered viable choices for microtubule-targeted cancer therapy. For example, the synthetic derivatives of noscapine called noscapinoids do not alter the polymer mass significantly but have been shown to possess high tumor specificity and negligible tissue toxicities (Lopus and Naik, 2015). Additionally, these congeners of the plant-derived alkaloid have been shown to be effective against multidrug-resistant cell lines. Similarly, the anti-tubulin agent dicoumarol only slightly reduces microtubule polymer mass but has been found to be a potential microtubule-targeted agent with strong anticancer potential (Madari et al., 2003). Estramsutine, an anticancer drug used in the treatment of prostate cancer, is another example of the tubulin-binding agents (Panda et al., 1997) that do not significantly alter microtubule polymer mass. A novel group of anti tubulin agents, taccalonolides, are also known for their ability to stabilize microtubule assembly (Risinger et al., 2013, 2014). β-SITO might not induce severe, dose-limiting toxicities, including peripheral nerve damage, because it does not significantly alter microtubule assembly dynamics. Drug-induced peripheral neuropathy is thought to arise due to severe disruption of microtubules in peripheral nerves caused by the chemotherapeutic agent (Miltenburg and Boogerd, 2014; Franker and Hoogenraad, 2013).

The direct binding of β-SITO to tubulin and the binding-induced alterations on the surface features of tubulin were confirmed with an ANS binding assay (Fig. 2). ANS non-covalently binds to hydrophobic amino acids on proteins and shows several-fold increases in fluorescence in its protein-bound state (Lopus and Panda, 2006). This method is routinely employed in studying the potential binding of microtubule assembly-modulating agents to tubulin.

After establishing that β-SITO stabilized tubulin assembly by binding to tubulin, we investigated further the nature of the interaction of β-SITO with tubulin. A colchicine binding assay showed that the compound did not bind at the colchicine site but, instead, stabilized colchicine binding, as indicated by the increase in colchicine fluorescence in the presence of the phytosterol (Fig. 3). The stabilization of colchicine binding by β-SITO suggested that its binding site might be in close proximity to the colchicine binding site. Interestingly, unlike the colchicine binding to tubulin that involves sulfhydryl groups, the binding of β-SITO to tubulin did not show involvement of –SH groups (Table 1). Many microtubule assembly-inhibiting compounds are known to interact with Cys residues, of which Cys 239 has been found to be the most reactive (Hamel, 2008). Therefore, it can be suggested that the observed lack of inhibition of microtubule assembly caused by β-SITO might be due to a lack of involvement of Cys residues in tubulin with β-SITO. However, it must be noted that a lack of involvement of Cys residues does not always result in the absence of inhibition of microtubule assembly. For example, pseudolarix acid B, a tubulin-binding anti-angiogenic agent, inhibits microtubule assembly without interacting with the sulfhydryl groups of tubulin (Tong et al., 2006).

4.2. Molecular modeling of β-SITO with tubulin

The data obtained from the biochemical assays formed the basis for the comprehensive computational modeling of β-SITO with tubulin. Tubulin provides binding sites for a number of ligands, and the drug-binding sites on tubulin are thought to be the binding sites for microtubule-associated proteins, including microtubule plus-end tracking proteins, such as EB1 and CLIP-170 (Lopus et al., 2012). As shown in the results section, ligand docking studies and a molecular dynamic simulation provided details of β-SITO binding to tubulin. While molecular docking indicated the putative binding site of the phytosterol, the simulation contributed to a detailed understanding of the binding of β-SITO to a αβ-tubulin complex in aqueous solution. Specifically, it was found that 9 amino acid residues (5 from β tubulin and 4 from α tubulin; Ala 99, Arg 104, Trp 406, Gly 409, Ile 162, Val 254, Pro 260, Arg 261, Leu 262; Fig. 5B, C and Table 4) were involved in the stabilization of the binding of β-SITO with tubulin. Notably, none of the amino acids present in the binding site of colchicine (Manchukonda et al., 2013) or vinblastine (Venghateri et al., 2013) were involved in the binding of β-SITO to tubulin. As well, none of the amino acids involved in noscapine binding to tubulin (at a site that partially overlapped the colchicine site) or in maytansine-tubulin interactions (Venghateri et al., 2013) were involved in β-SITO-tubulin interactions. Benomyl, a tubulin-binding benzimidazol, is thought to bind to tubulin at a novel site (Gupta et al., 2004). However, it is unlikely that β-SITO shares binding site with benomyl, whose binding to tubulin involves modification of cysteine residues (Gupta et al., 2004). Therefore, based on available information, we propose that β-SITO binds to a novel site on tubulin, which we call the SITO site. β-SITO stabilizes colchicine binding to tubulin; therefore, it can be assumed that the SITO site is in close proximity to the colchicine site. The docked location of β-SITO on tubulin (Fig 5A) supports this possibility.

4.3. Potential of β-SITO as a component in combination therapy

In facilitating microtubule assembly, β-SITO showed similarity to Taxol. Drugs that stabilize microtubules through different mechanisms have the potential to increase the effectiveness of individual drugs while minimizing their toxic side effects. For example, the combination of the microtubule-stabilizing agent estramustine with Taxol was found to be effective against hormone-refractory prostate cancer (Hudes et al., 1997). Similarly, another microtubule-stabilizing agent, dicoumarol, which is a coumarin anticoagulant, was found to be effective at inhibiting

cell division when combined with taxol (Madari et al., 2003). As discussed, β-SITO has functional biochemical similarities with estramustine and taxol. We propose that β-SITO has potential for use in combination therapy with taxol. Compounds such as taxol (Madari et al., 2003) and taccalonolides (Risinger et al., 2013, 2014) do not inhibit microtubule polymer mass but suppress the dynamic instability of microtubule (random alterations of the growth and shortening phases of microtubules; Yenjerla et al., 2010) and, thereby, disrupt mitotic spindle function, leading to mitotic arrest, often followed by cell death. β-SITO is known to disrupt cellular microtubules (Moon et al., 2008). It is possible that, at sub-stoichiometric concentrations, β-SITO also suppresses microtubule dynamic instability. Given the health benefits of β-SITO, including neuroprotection (Hamedi et al., 2014), this phytosterol is proposed as a suitable candidate for further pre-clinical and clinical evaluation as a potential anticancer drug.

Acknowledgment

The study was carried out with a financial support from UM-DAE Center for Excellence in Basic Sciences. We thank Dr. Jacinta D'Souza, UM-DAE CBS, for the use of the centrifuge and the Tecan multi-mode reader.

References

Awad, A.B., Chan, K.C., Downie, A.C., Fink, C.S., 2000. Peanuts as a source of β-sitosterol, a sterol with anticancer properties. Nutr. Cancer 36, 238–241. http://dx.doi.org/10.1207/S15327914NC3602_14.

Awad, A.B., Chen, Y.C., Fink, C.S., Hennessey, T., 1996. Beta-sitosterol inhibits HT-29 human colon cancer cell growth and alters membrane lipids. Anticancer Res. 16, 2797–2804.

Baskar, A.A., Ignacimuthu, S., Paulraj, G.M., Al Numair, K.S., 2010. Chemopreventive potential of beta-Sitosterol in experimental colon cancer model—an in vitro and in vivo study. BMC Complement. Altern. Med. 10, 24. http://dx.doi.org/10.1186/1472-6882-10-24.

Becke, A.D., 1993. A new mixing of Hartree–Fock and local density-functional theories. J. Chem. Phys. 98, 1372–1377.

Berendsen, H.J.C., Postma, J.P., van Gunsteren, W.F., DiNola, A., Haak, J.R., 1984. Molecular dynamics with coupling to an external bath. J. Chem. Phys. 81, 3684–3691. http://dx.doi.org/10.1063/1.448118.

Bhattacharyya, B., Wolff, J., 1974. Promotion of fluorescence upon binding of colchicine to tubulin. Proc. Natl. Acad. Sci. USA 71, 2627–2631.

Binkley, J.S., Pople, J.A., Hehre, W.J., 1980. Self-consistent molecular orbital methods. 21. Small split-valence basis sets for first-row elements. J. Am. Chem. Soc. 102, 939–947.

Bradford, M.M., 1976. A rapid and sensitive method for the quantitation of microgram quantities of protein utilizing the principle of protein-dye binding. Anal. Biochem. 72, 248–254.

Franker, M.A., Hoogenraad, C.C., 2013. Microtubule-based transport–basic mechanisms, traffic rules and role in neurological pathogenesis. J. Cell Sci. 126, 2319–2329.

Friesner, R.A., Banks, J.L., Murphy, R.B., Halgren, T.A., Klicic, J.J., Mainz, D.T., Repasky, M.P., Knoll, E.H., Shelley, M., Perry, J.K., Shaw, D.E., Francis, P., Shenkin, P.S., 2004. Glide: a new approach for rapid, accurate docking and scoring. 1. Method and assessment of docking accuracy. J. Med. Chem. 47, 1739–1749. http://dx.doi.org/10.1021/jm0306430.

Goodford, P.J., 1985. A computational procedure for determining energetically favorable binding sites on biologically important macromolecules. J. Med. Chem. 28, 849–857. http://dx.doi.org/10.1021/jm00145a002.

Gupta, K., Bishop, J., Peck, A., Brown, J., Wilson, L., Panda, D., 2004. Antimitotic antifungal compound benomyl inhibits brain microtubule polymerization and dynamics and cancer cell proliferation at mitosis, by binding to a novel site in tubulin. Biochemistry 43, 6645–6655. http://dx.doi.org/10.1021/bi036112v.

Gupta, K., Panda, D., 2002. Perturbation of microtubule polymerization by quercetin through tubulin binding: a novel mechanism of its antiproliferative activity. Biochemistry 41, 13029–13038.

Halgren, T.A., Murphy, R.B., Friesner, R.A., Beard, H.S., Frye, L.L., Pollard, W.T., Banks, J.L., 2004. Glide: a new approach for rapid, accurate docking and scoring. 2. Enrichment factors in database screening. J. Med. Chem. 47, 1750–1759.

Hamedi, A., Ghanbari, A., Saeidi, V., Razavipour, R., Azari, H., 2014. Effects of β-sitosterol oral administration on the proliferation and differentiation of neural stem cells. J. Funct. Foods 8, 252–258.

Hamel, E., 2008. An overview of compounds that interact with tubulin and their effects on microtubule assembly. In: Fojo, Tito (Ed.), The Role of Microtubules in Cell Biology, Neurobiology, and Oncology, 2008. Humana Press, New Jersey, pp. 1–19.

Hornak, V., Abel, R., Okur, A., Strockbine, B., Roitberg, A., Simmerling, C., 2006. Comparison of multiple Amber force fields and development of improved protein backbone parameters. Proteins 65, 712–725. http://dx.doi.org/10.1002/prot.21123.

Hudes, G.R., Nathan, F., Khater, C., Haas, N., Cornfield, M., Giantonio, B., Greenberg, R., Gomella, L., Litwin, S., Ross, E., Roethke, S., McAleer, C., 1997. Phase II trial of 96-hour paclitaxel plus oral estramustine phosphate in metastatic hormone-refractory prostate cancer. J. Clin. Oncol. 15, 3156–3163.

Jiménez-Escrig, A., Santos-Hidalgo, A.B., Saura-Calixto, F., 2006. Common sources and estimated intake of plant sterols in the Spanish diet. J. Agric. Food Chem. 54, 3462–3471. http://dx.doi.org/10.1021/jf053188k.

Kollman, P.A., Massova, I., Reyes, C., Kuhn, B., Huo, S., Chong, L., Lee, M., Lee, T., Duan, Y., Wang, W., Donini, O., Cieplak, P., Srinivasan, J., Case, D.A., Cheatham III, T.E., 2000. Calculating structures and free energies of complex molecules: combining molecular mechanics and continuum models. Acc. Chem. Res. 33, 889–897.

Lee, C., Yang, W., Parr, R.G., 1988. Development of the Colle-Salvetti correlation-energy formula into a functional of the electron density. Phys. Rev. B Condens. Matter 37, 785–789.

Lopus, M., Naik, P.K., 2015. Taking aim at a dynamic target: noscapinoids as microtubule-targeted cancer therapeutics. Pharmacol. Rep. 67, 56–62. http://dx.doi.org/10.1016/j.pharep.2014.09.003.

Lopus, M., Manatschal, C., Buey, R.M., Bjelić, S., Miller, H.P., Steinmetz, M.O., Wilson, L., 2012. Cooperative stabilization of microtubule dynamics by EB1 and CLIP-170 involves displacement of stably bound P(i) at microtubule ends. Biochemistry 51, 3021–3030. http://dx.doi.org/10.1021/bi300038t.

Lopus, M., Panda, D., 2006. The benzophenanthridine alkaloid sanguinarine perturbs microtubule assembly dynamics through tubulin binding. A possible mechanism for its antiproliferative activity. FEBS J. 273, 2139–2150. http://dx.doi.org/10.1111/j.1742-4658.2006.05227.x.

Lu, Y., Chen, J., Xiao, M., Li, W., Miller, D.D., 2012. An overview of tubulin inhibitors that interact with the colchicine binding site. Pharm. Res. 29, 2943–2971. http://dx.doi.org/10.1007/s11095-012-0828-z.

Madari, H., Panda, D., Wilson, L., Jacobs, R.S., 2003. Dicoumarol: a unique microtubule stabilizing natural product that is synergistic with Taxol. Cancer Res. 63, 1214–1220.

Manchukonda, N.K., Naik, P.K., Santoshi, S., Lopus, M., Joseph, S., Sridhar, B., Kantevari, S., 2013. Rational design, synthesis and biological evaluation of third generation α-noscapine analogues as potent tubulin binding anti-cancer agents. PLoS One 8, e77970. http://dx.doi.org/10.1371/journal.pone.0077970.

Massova, I., Kollman, P.A., 2000. Combined molecular mechanical and continuum solvent approach (MM–PBSA/GBSA) to predict ligand binding. Perspect. Drug Discov. Des. 18, 113–135. http://dx.doi.org/10.1023/A:1008763014207.

Miltenburg, N.C., Boogerd, W., 2014. Chemotherapy-induced neuropathy: a comprehensive survey. Cancer Treat. Rev. 40, 872–882. http://dx.doi.org/10.1016/j.ctrv.2014.04.004.

Moon, D.O., Kim, M.O., Choi, Y.H., Kim, G.Y., 2008. beta-Sitosterol induces G2/M arrest, endoreduplication, and apoptosis through the Bcl-2 and PI3K/Akt signaling pathways. Cancer Lett. 264, 181–191. http://dx.doi.org/10.1016/j.canlet.2008.01.032.

Panda, D., Miller, H.P., Islam, K., Wilson, L., 1997. Stabilization of microtubule dynamics by estramustine by binding to a novel site in tubulin: a possible mechanistic basis for its antitumor action. Proc. Natl. Acad. Sci. USA 94, 10560–10564.

Radika, M.K., Viswanathan, P., Anuradha, C.V., 2013. Nitric oxide mediates the insulin sensitizing effects of β-sitosterol in high fat diet-fed rats. Nitric Oxide 32, 43–53. http://dx.doi.org/10.1016/j.niox.2013.04.007.

Risinger, A.L., Li, J., Bennett, M.J., Rohena, C.C., Peng, J., Schriemer, D.C., Mooberry, S. L., 2013. Taccalonolide binding to tubulin imparts microtubule stability and potent in vivo activity. Cancer Res. 73, 6780–6792. http://dx.doi.org/10.1158/0008-5472.CAN-13-1346.

Risinger, A.L., Riffle, S.M., Lopus, M., Jordan, M.A., Wilson, L., Mooberry, S.L., 2014. The taccalonolides and paclitaxel cause distinct effects on microtubule dynamics and aster formation. Mol. Cancer 13, 41. http://dx.doi.org/10.1186/1476-4598-13-41.

Rosenblat, M., Volkova, N., Aviram, M., 2013. Pomegranate phytosterol (β-sitosterol) and polyphenolic antioxidant (punicalagin) addition to statin, significantly protected against macrophage foam cells formation. Atherosclerosis 226, 110–117. http://dx.doi.org/10.1016/j.atherosclerosis.2012.10.054.

Roychowdhury, M., Sarkar, N., Manna, T., Bhattacharyya, S., Sarkar, T., Basusarkar, P., Roy, S., Bhattacharyya, B., 2000. Sulfhydryls of tubulin. A probe to detect conformational changes of tubulin. Eur. J. Biochem. 267, 3469–3476. http://dx.doi.org/10.1046/j.1432-1327.2000.01369.x.

Ryckaert, J.P., Ciccotti, G., Berendsen, H.J.C., 1977. Numerical integration of the Cartesian equations of motion of a system with constraints: molecular dynamics of n-alkanes. J. Comput. Phys. 23, 327–341.

Saha, S.K., Khuda-Bukhsh, A.R., 2013. Molecular approaches towards development of purified natural products and their structurally known derivatives as efficient anti-cancer drugs: current trends. Eur. J. Pharmacol. 714, 239–248. http://dx.doi.org/10.1016/j.ejphar.2013.06.009.

Tong, Y.G., Zhang, X.W., Geng, M.Y., Yue, J.M., Xin, X.L., Tian, F., Shen, X., Tong, L.J., Li, M.H., Zhang, C., Li, W.H., Lin, L.P., Ding, J., 2006. Pseudolarix acid B, a new tubulin-binding agent, inhibits angiogenesis by interacting with a novel binding site on tubulin. Mol. Pharmacol. 69, 1226–1233. http://dx.doi.org/10.1124/mol.105.020537.

Venghateri, J.B., Gupta, T.K., Verma, P.J., Kunwar, A., Panda, D., 2013. Ansamitocin P3 depolymerizes microtubules and induces apoptosis by binding to tubulin at the vinblastine site. PLoS One 8, e75182. http://dx.doi.org/10.1371/journal.pone.0075182.

von Holtz, R.L., Fink, C.S., Awad, A.B., 1998. beta-Sitosterol activates the sphingomyelin cycle and induces apoptosis in LNCaP human prostate cancer cells. Nutr. Cancer 32, 8–12. http://dx.doi.org/10.1080/01635589809514709.

Vundru, S.S., Kale, R.K., Singh, R.P., 2013. β-Sitosterol induces G1 arrest and causes depolarization of mitochondrial membrane potential in breast carcinoma MDA-MB-231 cells. BMC Complement. Altern. Med. 13, 280. http://dx.doi.org/10.1186/1472-6882-13-280.

Wang, L., Yang, Y.J., Chen, S.H., Ge, X.R., Xu, C.J., Gui, S.Q., 2006. Effects of beta-sitosterol on microtubular systems in cervical cancer cells. Zhonghua Yi Xue Za Zhi 86, 2771–2775.

Wu, A.H., Ruan, W., Todd, J., Lynch, K.L., 2014. Biological variation of β-sitosterol, campesterol, and lathosterol as cholesterol absorption and synthesis biomarkers. Clin. Chim. Acta 430, 43–47. http://dx.doi.org/10.1016/j.cca.2013.12.040.

Yenjerla, M., Lopus, M., Wilson, L., 2010. Analysis of dynamic instability of steady-state microtubules in vitro by video-enhanced differential interference contrast microscopy. Methods Cell Biol. 95, 189–206. http://dx.doi.org/10.1016/S0091-679X(10)95011-5.

Yuk, J.E., Woo, J.S., Yun, C.Y., Lee, J.S., Kim, J.H., Song, G.Y., Yang, E.J., Hur, I.K., Kim, I.S., 2007. Effects of lactose-β-sitosterol and β-sitosterol on ovalbumin-induced lung inflammation in actively sensitized mice. Int. Immunopharmacol. 7, 1517–1527. http://dx.doi.org/10.1016/j.intimp.2007.07.026.

⟨http://www.accessdata.fda.gov/drugsatfda_docs/label/2009/022065s002lbl.pdf⟩.

⟨http://www.accessdata.fda.gov/drugsatfda_docs/label/2010/201532lbl.pdf⟩.

⟨http://www.accessdata.fda.gov/drugsatfda_docs/label/2013/125427lbl.pdf⟩.